

Flexibility Framework with Recovery Guarantees for Aggregated Energy Storage Devices

Michael P. Evans, Simon H. Tindemans, *Member, IEEE* and David Angeli, *Fellow, IEEE*

Abstract—This paper proposes a framework for the procurement of flexibility reserve from aggregated storage fleets. It allows for arbitrary tree structures of aggregation hierarchy, as well as easily implementable disaggregation via broadcast dispatch. By coupling discharge and recovery modes, the proposed framework enables full-cycle capacity to be procured ahead of real time, with guaranteed recovery and exact accounting for losses. The set of feasible discharging requests is exactly encoded, so that there is no reduction in the ability to meet discharging signals, and recovery capabilities are parametrised as a single virtual battery. Included in this paper is a numerical demonstration of the construction of the constituent curves of the framework and the approach is also benchmarked against relevant alternatives.

Index Terms—Aggregation, virtual power plant, energy storage systems, optimal control, ancillary service, virtual battery

I. INTRODUCTION

Recent years have seen an increased proliferation of renewable energy sources onto electricity networks, leading to increased difficulty in the task of balancing supply and demand. Energy storage units offer significant potential in addressing this imbalance; for example National Grid, the Electricity System Operator, predicts that between 28 and 75 GW of electricity storage (including vehicle-to-grid) capacity will be used to balance the British network by 2050 [1]. Prior literature on ancillary services has covered multiple classes of storage device, such as EV batteries [2]–[7], diesel generators [8], [9] and home storage units [3], [10]–[13]; and a battery model can even capture the properties of a time-shift in electrical load [14]. The total capabilities of units that can be modelled as batteries is therefore very significant.

A key enabling technology for large numbers of devices to participate in balancing frameworks is their *aggregation*. This combination of individual units into compound entities, often termed Virtual Power Plants, offers a useful abstraction framework: in amalgamating a complex fleet into a single capability representation, one can consider there to be a single service provider. This leads to ease of interaction with the service user, as well as a reduction in the direct communication infrastructure connecting individual device owners and the user.

M.P. Evans completed the majority of this work while with the Department of Electrical and Electronic Engineering, Imperial College London, UK. He is currently with Octopus Energy, UK (email: michael.p.evans21@gmail.com). S.H. Tindemans is with the Department of Electrical Sustainable Energy, TU Delft, Netherlands and was affiliated with the Alan Turing Institute, UK when the research was performed (email: s.h.tindemans@tudelft.nl). D. Angeli is with the Department of Electrical and Electronic Engineering, Imperial College London, UK, and the Department of Information Engineering, University of Florence, Italy (email: d.angeli@imperial.ac.uk). Corresponding author: S.H. Tindemans.

Multiple authors have considered the aggregation of energy storage units [4]–[7], [14], [15]. The predominant form of aggregation has been the summation of power and energy limits across devices, as exemplified by [5]. While this functions as intended for homogeneous fleets, we showed in [16] that such a representation only serves to outer-bound the true flexibility limits of a heterogeneous device pool. The summation-aggregation approach was improved upon in [4], where Vandael *et al.* presented a receding horizon version of the summed parameter model, with the addition of necessary constraints on total charge profiles; this same tightening of the aggregate energy constraints was then applied in [6], [7]. However, the retention of a summed power limit allowed the fleet to run at full power up to the point of full charge (equivalent to energy depletion in a discharging setting). When such an aggregation approach is utilised to compose constraints on an optimisation problem, this can still lead to the allocation of infeasible requests. Appino *et al.* noted this shortfall of summation based aggregation in [15]. While our approach is to directly rectify this problem, they instead imposed conditions so that a summation was able to exactly capture the flexibility limits of the fleet. In doing so, these conditions necessarily restrict the aggregate flexibility, however, which may result in sub-optimal allocation when a feasible optimum is placed outside of the considered region. By contrast, the control approach presented in [16] was able to exactly capture aggregate discharging capabilities. There, we presented a transform which exactly encodes fleet flexibility, under the restriction to unidirectional operation and a lack of cross-charging, termed the E - p transform. This is the predominant tool that we will use in our analysis here, applied to coupled discharge-recharge operation. An equivalent fleet flexibility measure was presented by Cruise and Zachary in [17].

In addition to the aforementioned benefits, aggregation (either directly or in stages) also enables an anonymisation of individual unit owners. Moreover, where device availability is stochastic, the aggregation of units leads to a statistical smoothing of the overall behaviour, i.e. a robustification of the net output. For example, chance constraints can be applied to achieve an arbitrary risk level (as in [18]) only on aggregate.

Network operators are increasingly offering frameworks for balancing services, procured through ancillary service markets (e.g. [19]–[21]). Once these markets exist, they encourage the formation of complex ecosystems in which entities of various types and sizes exchange arbitrary ancillary service provisions with one another. In this regard, a desirable feature in an aggregation scheme is the ability to abstract the capabilities

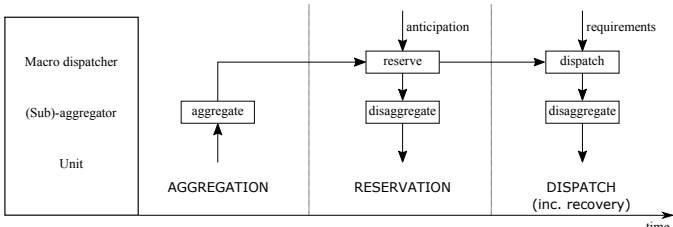


Fig. 1: The separation in time of aggregation, reserve scheduling and dispatch according to the presented framework.

of a fleet in such a way that aggregates themselves can be combined into larger aggregates. This property enables hierarchical aggregation, which improves scalability and underpins combination and re-packaging of services. Examples of such hierarchical aggregation schemes exist in related fields. For example, for thermostatically controlled loads, aggregate capability representations were presented in [22], [23] and then combined using Minkowski summation in [24]. A similar geometric addition was presented for active-reactive power (P - Q) flexibility in [25]. To our knowledge, however, there currently exists no comparable method for the aggregation of power-energy flexibilities of heterogeneous storage fleets.

A particular challenge when deploying demand response services is the need to schedule recovery (or recharging in the case of batteries), potentially under a strict deadline. O’Connell *et al.* [14] proposed asymmetric block offers as a means of co-optimising response and rebound in a single operation. By packaging response and rebound (or equivalently discharging and recharging) into a single offer, they guarantee full recovery at a specified time, thus reducing risk exposure.

This paper introduces a framework for hierarchical aggregation of heterogeneous storage fleets that guarantees energy recovery: the *discharge-loss-recovery* (DLR) framework. This addresses the same challenge as [14], but extends the approach in two important ways: first, in place of a virtual battery, the DLR representation precisely encodes the aggregate capabilities of heterogeneous storage units. Second, instead of a discrete set of offers, a continuous set of capabilities is communicated. This framework therefore enables ahead-of-time scheduling without sacrificing achievability or recovery. As such, it enables a macro dispatcher (e.g. a system operator) to reserve flexibility in a consistent way, bounding the operational risk (and reducing associated costs) as compared to transmitting emergency requests in real time. This results in the three-stage process shown in Figure 1. At present, there are three major use-cases for ahead-of-time reservation of flexibility: 1) grid balancing, contracted by the TSO; 2) portfolio balancing, contracted by balance responsible parties; and 3) congestion management, contracted by DSOs.

The DLR framework encodes the flexibility of storage units for the (sub-)aggregators and the macro-dispatcher, and incorporates dispatching of these units. It offers the following properties:

- Accounting for heterogeneity of storage units and round-trip losses.
- Exact encoding of aggregate discharge flexibility.
- Assuming maximum discharge flexibility, *a priori* determination of recovery requirements (energy and minimum recharge time).

- Hierarchical aggregation of flexibility and disaggregation via broadcast dispatch.

Reflecting the predominant use of storage under supply-shortfall conditions today, we focus on discharging requests followed by recharging recovery. The presented technique can then be applied to the opposite case via a straightforward inversion of the coordinate system used.

II. PROBLEM DESCRIPTION

A. Mathematical description

As our focus is on the ability of a fleet to counter supply-shortfall conditions, we frame the problem based on discharging operation, and choose the convention that discharging power outputs are positive. We denote the constituent heterogeneous units of the fleet as D_i , $i = 1, \dots, n$, each with extractable energy $e_i(t)$ subject to the assumed physical constraint $0 \leq e_i(t) \leq \bar{e}_i$. We choose as our control input $u_i(t)$ the power extracted from each device, measured externally so as to take into account any inefficiencies present during discharging operation. This then leads to the following integrator dynamics:

$$\dot{e}_i(t) = \begin{cases} -u_i(t), & \text{if } u_i(t) \geq 0 \\ -\eta_i u_i(t), & \text{otherwise,} \end{cases} \quad (1)$$

in which $\eta_i \in [0, 1]$ denotes the round-trip efficiency of device D_i .

We assume a lack of cross-charging, by which we mean the use of available headroom to redistribute energy among devices.¹ During discharging operation, we denote the power limits of each device as $u_i(t) \in [0, \bar{p}_i]$. We choose as our state variable the *time-to-go*, defined for each device as $x_i(t) \doteq e_i(t)/\bar{p}_i$. We then stack state, input and maximum power values across devices as follows:

$$x(t) \doteq [x_1(t) \ \dots \ x_n(t)]^T, \quad (2)$$

$$u(t) \doteq [u_1(t) \ \dots \ u_n(t)]^T, \quad (3)$$

$$\bar{p} \doteq [\bar{p}_1 \ \dots \ \bar{p}_n]^T, \quad (4)$$

allowing us to rewrite the discharging dynamics in matrix form as $\dot{x}(t) = -P^{-1}u(t)$, in which $P \doteq \text{diag}(\bar{p})$. We also form the product set of the power constraints, $\mathcal{U}_{\bar{p}} \doteq [0, \bar{p}_1] \times [0, \bar{p}_2] \times \dots \times [0, \bar{p}_n]$, so that our discharging constraints can be compactly written as $u(t) \in \mathcal{U}_{\bar{p}}$ and $x(t) \geq 0$.

B. Feasibility and flexibility

The intention of this paper is to present a framework through which a macro dispatcher can procure flexibility reserve, ahead of real-time dispatch of the reserved capabilities. This generalises the concept of a two-stage scheduling-dispatch routine (see [16] for further details), since the reserve circumscribes the set of admissible schedules. For consistency, then, it is imperative that the considered framework encodes those

¹It is shown in [26] that cross-charging does not increase the feasible set for fully charged storage devices serving a unimodal signal. Moreover, cross-charging of devices with less than 100% efficiency necessarily results in a loss of energy, which is often undesirable.

schedules that are *feasible*, by which we mean that they do not violate any physical device constraints. Initially, we focus our attention on pure discharging requests, which we allocate as positive by convention and denote¹ by $P^d: [0, +\infty) \mapsto [0, +\infty)$. We then characterise the set of feasible requests and define flexibility as follows:

Definition II.1. The *feasible set* of discharging requests, for a system with maximum power vector \bar{p} and initial state $x = x(0)$, is defined as

$$\mathcal{S}_{\bar{p},x} \doteq \left\{ P^d(\cdot) : \exists u(\cdot), z(\cdot) : \forall t \geq 0, 1^T u(t) = P^d(t), \right. \\ \left. u(t) \in \mathcal{U}_{\bar{p}}, \dot{z}(t) = -P^{-1}u(t), z(0) = x, z(t) \geq 0 \right\}.$$

By contrast, we define the *flexibility* as follows:

Definition II.2. The *flexibility* of an energy resource is an encoding of the feasible set that has the following properties

- 1) A numerical representation of admissible requests
- 2) An accompanying dispatch routine to realise admissible requests
- 3) Guaranteed feasibility of each admissible request within a priori bounds

We say that flexibility is maximised if the bounds on admissible signals exactly encode the feasible set, thus guaranteeing feasibility without restricting the operational envelope.

C. The E - p transform

We presented an example of flexibility maximisation in [16], precipitated through the restriction to pure discharging operation, termed the E - p transform. We will utilise this here and so make the following reproductions:

Definition II.3. Given a discharging power request $P^d(\cdot)$, we define its E - p transform as the following function:

$$E_{P^d}(p) \doteq \int_0^\infty \max\{P^d(t) - p, 0\} dt,$$

interpretable as the energy required above any given power rating, p . The E - p transform is convex and monotone.

Definition II.4. We define the discharge *capacity* of a system to be the E - p transform of the worst-case request that it can meet, i.e.

$$\Omega_{\bar{p},x}(p) \doteq E_{R_{\bar{p},x}}(p),$$

with $R_{\bar{p},x}(t) \doteq \sum_{i=1}^n \bar{p}_i [H(t) - H(t - x_i)]$, in which $H(\cdot)$ denotes the Heaviside step function.

Property II.5. A discharging request $P^d(\cdot)$ is feasible if, and only if, its E - p transform is dominated by the capacity of the system, i.e. $P^d(\cdot) \in \mathcal{S}_{\bar{p},x} \iff E_{P^d}(p) \leq \Omega_{\bar{p},x}(p) \forall p$.

A graphical example of the use of the E - p transform, via Property II.5, as a binary feasibility check can be seen in Figure 2. We reiterate that, under enforced conditions, the capacity curve exactly encodes the feasible set. We can therefore formally define the corresponding flexibility as follows:

¹In the interest of clarity, some of the notation used here will differ from that of our prior work [16], [18], [27], [28]

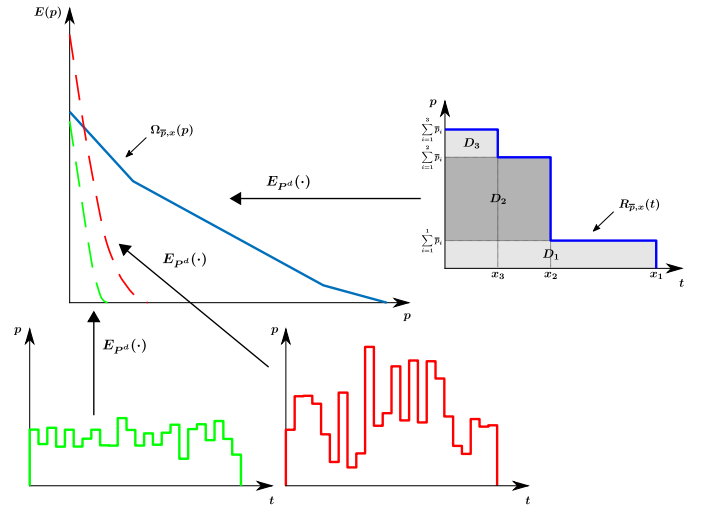


Fig. 2: An example use of the E - p transform as a binary feasibility check, implementing Property II.5. The capacity curve is formed based on fleet parameters, and received requests are transformed into E - p space; at which point the binary feasibility check can be made by eye. The green curve is found to be feasible, while the red curve is found to be infeasible.

Definition II.6. The *pure discharging flexibility* of a fleet with maximum power vector \bar{p} in state x is defined as

$$\mathcal{F}_{\bar{p},x} \doteq \left\{ (p, E) : p \geq 0, E \leq \Omega_{\bar{p},x}(p) \right\} \\ = \left\{ (p, E_{P^d}(p)) : p \geq 0, P^d(\cdot) \in \mathcal{S}_{\bar{p},x} \right\}.$$

It also has the following property that will be useful in our analysis:

Property II.7. The complement to the discharging fleet flexibility, $\mathcal{F}_{\bar{p},x}^c = ([0, +\infty) \times [0, +\infty)) \setminus \mathcal{F}_{\bar{p},x}$, is a convex set.

D. Default dispatch policy

In [27], we presented a policy and showed it to maximise the flexibility of the fleet at all future time instants. We then presented a discrete time equivalent to this in [28], which allocates a piecewise constant control input to match a piecewise constant request. In our framework, we will utilise the latter for default dispatch and therefore reproduce it here as follows. We restrict ourselves to a constant dispatch period Δt , envisioning that this will be most relevant in practical settings. Given a request that takes a constant value P^d across the time interval, a target state value \hat{z} is found as

$$\hat{z} : \sum_{i=1}^n \bar{p}_i \max\{0, \min\{x_i - \hat{z}, \Delta t\}\} = P^d \Delta t, \quad (5a)$$

then the input is constructed according to

$$u_i = \bar{p}_i \cdot \max\left\{0, \min\left\{\frac{x_i - \hat{z}}{\Delta t}, 1\right\}\right\}, \quad (5b)$$

resulting in time-to-go updates

$$x_i \leftarrow x_i - \frac{u_i \Delta t}{\bar{p}_i}. \quad (5c)$$

Note that the algorithm is applied at each time step, so explicit time-dependence is omitted. Also, unlike in [28], we need only consider feasible requests, which leads to equality in the energy balance of (5a).

E. Symmetry to recharging operation

Up to this point, we have considered pure discharge operation. We will now extend this to the recharging of devices between shortfall events. We denote a recharging request as $P^r: [0, +\infty) \mapsto (-\infty, 0]$. Analogous to time-to-go, we utilise the *time-to-charge*, defined as follows:

$$y_i(t) \doteq \frac{\bar{e}_i - e_i(t)}{\eta_i \underline{p}_i}, \quad (6)$$

in which \underline{p}_i denotes the (magnitude of the) maximum charge rate of device D_i . Equivalently, this can be obtained from a time-to-go value via the following change of (instantaneous) variables:

$$y_i = \frac{\bar{p}_i(\bar{x}_i - x_i)}{\eta_i \underline{p}_i}, \quad (7)$$

in which $\bar{x}_i \doteq \bar{e}_i/\bar{p}_i$ is the maximum time-to-go value of device D_i . When considering pure recovery operation, then, we are able to perform the conversions $x_i \rightarrow y_i$, $P^d \rightarrow -P^r$, $\bar{p}_i \rightarrow \underline{p}_i$ and $u_i \rightarrow -u_i^r$, where u^r denotes the (negative) control input while recharging, and the equivalent results hold.

Just as the scheduling from an arbitrary state can be considered in either direction, the corresponding default dispatch policy will be given by either (5) or its equivalent in terms of time-to-charge. The user is alternatively able to compose the recharging policy based directly on discharging parameters as follows. Given a request that takes a constant value P^r across the time interval Δt , a target (recharging) state value \hat{y} is found as

$$\hat{y} : \sum_{i=1}^n \underline{p}_i \max \left\{ 0, \min \left\{ \frac{\bar{p}_i(\bar{x}_i - x_i)}{\eta_i \underline{p}_i} - \hat{y}, \Delta t \right\} \right\} = -P^r \Delta t, \quad (8a)$$

then the input is constructed according to

$$u_i^r = -\underline{p}_i \cdot \max \left\{ 0, \min \left\{ \frac{\bar{p}_i(\bar{x}_i - x_i) - \eta_i \underline{p}_i \hat{y}}{\eta_i \underline{p}_i \Delta t}, 1 \right\} \right\}, \quad (8b)$$

resulting in time-to-go updates

$$x_i \leftarrow x_i - \frac{\eta_i u_i \Delta t}{\bar{p}_i}. \quad (8c)$$

III. THE DLR FRAMEWORK

A. Sequential versus integrated scheduling

Our intention is to construct a single flexibility representation that encodes the feasible set (under no cross-charging) for the full discharge-recovery cycle. This then allows for scheduling of the complete cycle ahead of real-time.

We restrict our analysis to requests that are positive or zero (discharging) over some period, followed by negative or zero (recharging) over another period, such that full recharging of all devices is achieved; this cycle can then be repeated. We do not explicitly limit the duration of either period, but such a constraint can be communicated as an additional parameter. In line with the previous section, we shall denote a discharge-recovery request as $P^d \oplus P^r(\cdot)$, in which the \oplus operator denotes the concatenation of two signals.

The results in Section II provide the tools to implement a two-stage solution to this problem. First, the discharging

capacity curve (which, to emphasise the mode, we denote as $\Omega^d(\cdot) \doteq \Omega_{\bar{p},x}^d(\cdot)$) is used to determine feasibility of a discharge request $P^d(\cdot)$, and the dispatch policy (5) used to realise it. Then, the procedure is repeated for the recharge request $P^r(\cdot)$. However, the *recharge capacity curve* $\Omega^r(\cdot)$ and, importantly, the total amount of energy required to recharge while accounting for losses, depend on the terminal state of charge of the storage units after the discharge operation, which in turn depends on (the E-p transform of) the discharge signal $P^d(\cdot)$. This dependency hinders the formulation of a compact flexibility representation that incorporates recharging.

B. The DLR flexibility representation

In this section, we introduce a representation of the set of feasible integrated discharge-recovery schedules that has the following properties:

- It maximises the discharging flexibility, so that the set of considered discharging signals exactly matches the feasible set.
- It exactly accounts for round-trip losses in the recharging phase. This is a crucial requirement for any aggregation method used to produce constraints on an optimisation problem.
- It returns recharge parameters in the form of a simple virtual battery model, characterised by recharge energy and minimum time-to-charge (equivalently recharge power and energy ratings).

As mentioned in the previous section, the recharge requirements depend on the terminal state of the discharge procedure. In order to simplify the description of recharge flexibility, we introduce a one-dimensional parameterisation of the discharging flexibility as a function of the total energy requirement E^d , in such a way that discharging flexibility is not sacrificed and an exact encoding of the recharge requirements is possible. This representation reduces the feasible set of recharging patterns, in exchange for a compact representation that facilitates pre-scheduling of recharging.

The proposed *discharge-loss-recovery time* (DLR) representation consists of three 1-parameter functions:

- D) The *discharge* capacity curve $\Omega^d(\cdot)$ (Definition II.4);
- L) The *loss* function, describing the energy required to recharge as a function of the discharge energy E^d ;
- R) The *recovery time* function, describing the minimum time required to recharge as a function of the discharge energy E^d .

Together, the loss and recovery functions define the E^d -dependent parameters of a single virtual battery for recharging. The DLR representation is illustrated in Figure 3. Details on the construction of the DLR-curves are provided in the remainder of this section.

C. Discharging capacity and guaranteed final state

The first element of the DLR representation, the *discharging capacity* is given by the capacity curve $\Omega^d(\cdot)$, which exactly encodes the feasible set of discharging signals.

Given a feasible discharge signal $P^d(\cdot)$ and an initial state, the dispatch strategy (5) determines the terminal state of

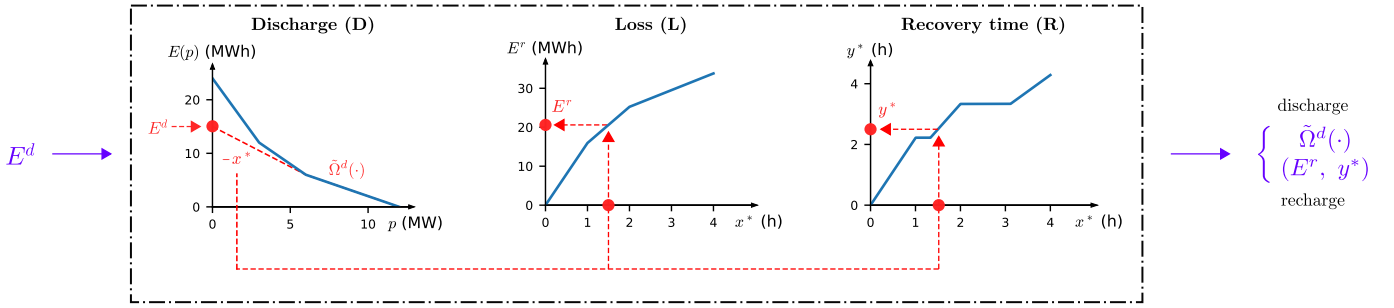


Fig. 3: Constructing discharging and recovery flexibilities based on a DLR packet and a total energy E^d , with construction lines shown in dashed red.

charge of each storage unit. In order to reduce the space of possible outcomes without limiting feasibility, we construct a *maximum-flexibility truncated fleet* that limits the time-to-go of each storage unit. This truncated fleet is parameterised by E^d and will be exactly emptied during discharge operation and refilled during recovery, *without* restricting the feasible set conditioned on the discharged energy E^d . For a given fleet of power rating \bar{p} in state x , we define

$$\tilde{x}_i = \min\{x_i, x^*\}, \quad i = 1, \dots, n, \quad (9a)$$

in which x^* is defined according to

$$x^*(E^d) : \sum_{i=1}^n \bar{p}_i \min\{x_i, x^*\} = E^d. \quad (9b)$$

This truncated fleet construction satisfies the following result, the proof of which can be found in the Appendix:

Theorem III.1. *Given a request profile $P^d(\cdot)$ and a fleet with maximum power vector \bar{p} in state x ,*

$$P^d(\cdot) \in \mathcal{S}_{\bar{p}, x} \iff P^d(\cdot) \in \mathcal{S}_{\bar{p}, \tilde{x}}, \quad (10)$$

in which \tilde{x} is defined according to (9) with $E^d \geq \int_0^\infty P^d(t) dt$.

Thus, in the knowledge that $P^d(\cdot)$ will have a total energy no greater than E^d , the original fleet can be replaced by a truncated fleet, using (9), and maintain its ability to meet considered signals. Moreover, if the total energy provided *exactly* equals E^d , then the virtual fleet will be emptied and the true fleet is in a known state, regardless of the distribution of power levels in $P^d(\cdot)$. This property gives the sought reduction in recharge complexity.

Theorem III.1 also leads to the following Corollary:

Corollary III.2. *The flexibility of a truncated fleet as in (9) can be found as*

$$\mathcal{F}_{\bar{p}, \tilde{x}}^{\mathcal{C}} = \text{Conv}(\mathcal{F}_{\bar{p}, x}^{\mathcal{C}} \cup \{(0, E^d)\}), \quad (11)$$

in which $\text{Conv}(\cdot)$ denotes the convex hull operator.

This result gives us a means to construct the capacity curve of the truncated fleet directly from a full capacity curve, without considering constituent devices. Figure 4 demonstrates this graphically where, for simplicity of notation, we define $\tilde{\Omega}^d(\cdot) \doteq \Omega_{\bar{p}, \tilde{x}}^d(\cdot)$. We note that, by construction, the discharge capacity curve of the truncated fleet has the property

$$\left. \frac{d\tilde{\Omega}^d(p)}{dp} \right|_{p=0^+} = -x^* \quad (12)$$

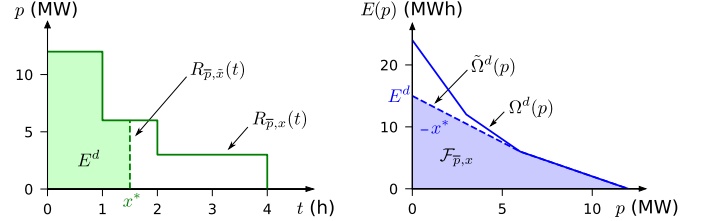


Fig. 4: The correspondence between the worst-case request (left panel) and capacity curve (right panel) for a truncated fleet formed as in (9). The green shaded area is equal to the total requested energy, while the discharging flexibility is shaded in blue.

D. Loss and recovery time functions

Recall that a discharge request with energy E^d will exactly empty an E^d -truncated virtual fleet. The total energy required to recharge is therefore given by

$$E^r(x^*) = \sum_{i=1}^n \frac{\bar{p}_i}{\eta_i} \min\{x_i, x^*\}, \quad (13)$$

with x^* as in (9b). We term this the *loss function* and note that it is piecewise linear, with n sections in general, and concave.²

The third and final component of the DLR representation is the *recovery time function*. The initial recharge state corresponds to the truncated fleet being exactly depleted. The fastest recovery is determined by the largest time-to-charge value, which is therefore given by

$$y^*(x^*) \doteq \max_{i \in \{1, \dots, n\}} \frac{\bar{p}_i}{\eta_i \bar{p}_i} \min\{x_i, x^*\}, \quad (14)$$

with x^* as in (9b). This function is monotone and piecewise linear, with $2n - 1$ sections in general.

Together, $E^r(x^*)$ and $y^*(x^*)$ describe a virtual storage unit. Acceptable recharging profiles $P^r(\cdot)$ must fully recharge this unit by supplying an amount of energy E^r subject to a maximum power rating E^r/y^* . As it can be seen in Figure 3, then, the constituent DLR curves are sufficient to encode, for a given total discharge energy, coupled discharging and recharging flexibilities. These guarantee feasibility of any allocated request, and as such the DLR representation should be considered a consistent flexibility metric for integrated discharge-recovery operation.

²The loss and recovery time functions could alternatively be parameterised by E^d in place of x^* . The derivative of the loss function, i.e. $\frac{dE^r}{dE^d}$, would then be a p -weighted average of $1/\eta$ of participating batteries. However, we opt for x^* here for increased convenience of aggregation and broadcast.

We also point out here that, in the special case where all devices have the same round-trip efficiency and ratio of charging/discharging rates, implementation of the default discharging policy maximises charging flexibility for a given total energy. Hence, when these parameter conditions apply, full-cycle flexibility is maximised in the sense that the recharge energy and recharge time are minimal for a given discharge energy E^d .

IV. AGGREGATION, RESERVATION AND DISPATCH

The framework that we present enables the separation in time of aggregation, flexibility reservation and dispatch, as was shown in Figure 1. Having presented the elements required for implementation of this framework, we here provide details on each of the three constituent time periods, in Figure 5 and the following subsections.

A. Aggregation

The DLR representation is computed on the basis of the fleet parameter tuple (\bar{p}, x, p, η) (each vector-valued). It is then straightforward to see that DLR representations can be combined: by converting each back to fleet parameters (one virtual device per unique time-to-go value), amalgamating all of these and finally forming a single compound DLR packet. This framework therefore implicitly allows for aggregation in arbitrary hierarchies.

We would, however, like to achieve the combination of DLR packets based directly on the three constituent curves, i.e. without reverting to device parameters. Without loss of generality, we consider the aggregation of two fleets with parameters $(\bar{p}^{(1)}, x^{(1)}, p^{(1)}, \eta^{(1)})$ and $(\bar{p}^{(2)}, x^{(2)}, p^{(2)}, \eta^{(2)})$. To reduce clutter, we simplify notation by using only the subscript 1 or 2 to summarise the respective quantities. Each of the three DLR curves is treated in one of the following subsections.

1) *Discharge capacity curve:* We initially consider discharge flexibilities, for which we are able to derive the following result (proof in the Appendix):

Theorem IV.1. *The **discharging flexibility** of an aggregate fleet can be computed by the following complementary Minkowski summation:*

$$\mathcal{F}_{1+2}^{\mathbb{C}} = (\mathcal{F}_1^{\mathbb{C}} \oplus \mathcal{F}_2^{\mathbb{C}})^{\mathbb{C}}. \quad (15)$$

This then leads directly to the following result:

Corollary IV.2. *Capacity curves can be added as follows:*

$$\Omega_{1+2}(p) = \sup\{E: (p, E) \notin \mathcal{F}_1^{\mathbb{C}} \oplus \mathcal{F}_2^{\mathbb{C}}\}. \quad (16)$$

The combined capacity curve $\Omega_{1+2}(p)$ also defines the fleet truncation parameter $x^*(E^d)$ through (12).

2) *Loss function:* A time-to-go value x^* defines all individual device recharge energy needs, regardless of their grouping into fleets. Hence the total energy requirement can be found via a simple pointwise summation, i.e.

$$E_{1+2}^r(x^*) = E_1^r(x^*) + E_2^r(x^*). \quad (17)$$

3) *Recovery function:* The minimum recovery time is set by the largest time-to-charge value. As such, when two curves are amalgamated, it is the maximum of these values that determines the minimum recharge time, i.e.

$$y_{1+2}^*(x^*) = \max\{y_1^*(x^*), y_2^*(x^*)\}. \quad (18)$$

Finally, we remark that the DLR representation of a fleet can be constructed in this way by aggregating DLR representations of elementary storage units, each given by:

$$\Omega_{\text{single}}(p) = \bar{e}(1 - p/\bar{p}) \quad (19a)$$

$$E_{\text{single}}^r(x^*) = \frac{\bar{p}}{\eta} \min\{x, x^*\} \quad (19b)$$

$$y_{\text{single}}^*(x^*) = \frac{\bar{p}}{\eta p} \min\{x, x^*\} \quad (19c)$$

B. Flexibility reservation

Without loss of generality, we assume that the macro dispatcher has a direct communication link to a number of top-level aggregators. Once it has received all DLR capabilities, compound or otherwise, we envision that the macro dispatcher makes a decision as to what flexibility provision to reserve from each; and we place no restrictions on the method through which this is chosen. Once this decision has been made, the actual reservation takes place through the transmission of the amount of reserved energy (one value: E^d) to each top-level aggregator. Each of these then calculates the corresponding x^* -value, which it broadcasts among its fleet. Once reservation has been realised through the allocating of x^* values, a truncated fleet is formed as each unit sets its virtual initial state $\tilde{x}_i = \min\{x_i, x_i^*\}$; this virtual device will be fully discharged and recharged. We point out here that dispatch via the policy (5) ensures participation of all units, and hence so too does the allocation of devices under the proposed framework.

As an extension to this reservation method, the aggregator could in fact amend the truncation level of each device and/or the dispatch strategy, so long as the aggregate constraints were met; in this case it would broadcast a vector x^* of length n instead. However, this is not further investigated here.

C. Broadcast dispatch

The DLR construction is such that any admissible signal can necessarily be met by the implementation of the policy (5) and its equivalent for recharging. Under this combined policy, each device solely requires the \hat{z} value corresponding to each request level in order to allocate its output. Moreover, this remains true regardless of the grouping of devices into fleets. As a result, the framework that we propose directly enables broadcast dispatch. There is no need to cascade signals down the tree; rather, each top-level aggregator can broadcast a single \hat{z} level and the units will respond accordingly.

D. Benefits of the combined framework

We consider this approach to be *scalable* (c.f. [4]), based on its combination of arbitrary aggregation hierarchy and broadcast dispatch. From their construction according to a fleet

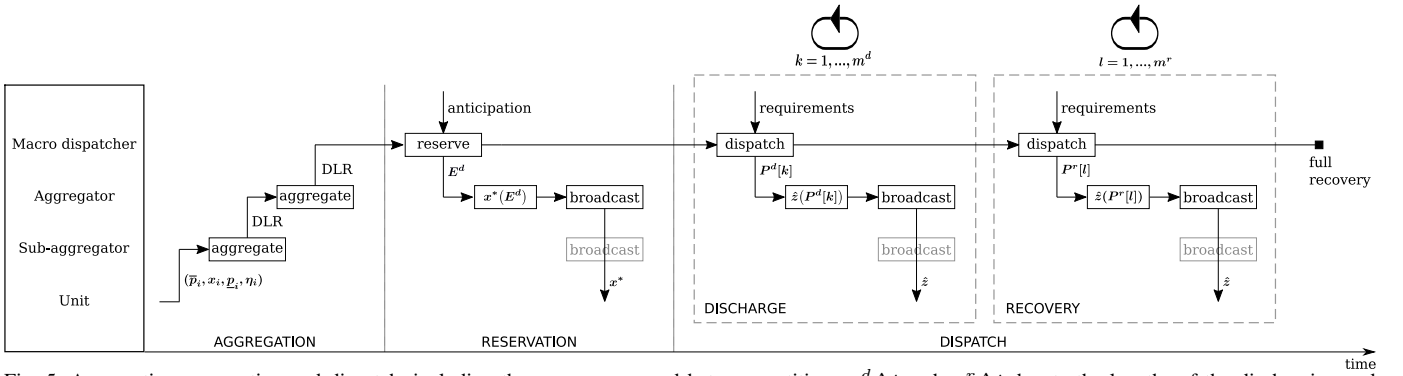


Fig. 5: Aggregation, reservation and dispatch, including the messages passed between entities. $m^d \Delta t$ and $m^r \Delta t$ denote the lengths of the discharging and recharging periods, respectively. Transparent boxes show optional disaggregation steps at one or more sub-aggregator levels.

TABLE I: Benchmarking the DLR framework against alternative dispatch approaches. Green cells are preferred over orange, which are in turn preferred over red. Within the green cells, dark green denote an improvement over light green.

Approach	discharging flexibility	advance commitment	energy recovery	recharging flexibility	aggregation of products	visual representation of flexibility	dispatch method
DLR framework	full*	discharge energy	exact, in advance	minimum time	yes	yes	broadcast
Sequential E - p dispatch	full	none	exact, after discharge	full	yes	yes	broadcast
Single virtual battery**	limited, continuous	none	not guaranteed	limited, continuous	no	yes	implementation dependent
Asymmetric block offers	limited, options given	full	exact, in advance	limited, options given	no	yes	implementation dependent
Full information scheduling	full	full	exact, in advance	full	yes	no	direct, ahead of time
Full information direct control	full	none	exact, full control	full	yes	no	direct, real time

* with the exclusion of cross-charging as discussed in Section II.

** parameters chosen to ensure feasibility in both directions.

of discrete devices, each of the three DLR curves are piecewise linear. As a result, we envision that these metrics are passed between entities as vectors of their vertices; the lengths of these will scale as $\mathcal{O}(n)$.

Guaranteed recovery also means that multiple DLR packets can be sold ahead of operation for sequential use. The macro dispatcher need not fully utilise each DLR packet; in fact, it need not call upon it at all if the realised net demand does not exceed supply. Two options exist for a partial utilisation of a purchased DLR packet: 1) between discharging and recharging operation, update E^r (retain y^* even though it may lead to an unnecessarily conservative rate constraint); 2) before the start of the operational period, allow for scheduling updates to reduce E^d and accordingly x^* .

V. EXAMPLE USES OF THE DLR FRAMEWORK

A. Numerical demonstration

We now demonstrate construction of the DLR curves for a numerical example. Consider the fleet with parameters given in Table II, so that $n = 3$ and the other parameters are such that the maximum number of linear sections is observed on each of the discharge, loss and recovery time curves: 3, 3 and 5 respectively. These curves can be seen in Figures 3 and 4.

TABLE II: Parameters for the three-battery example

Battery #	Parameter			
	\bar{p}_i (MW)	x_i (h)	\underline{p}_i (MW)	η_i (%)
1	3	4	4	70
2	3	2	3	60
3	6	1	3	90

B. Benchmarking the DLR framework

We next benchmark the DLR framework against the state-of-the-art in optimal scheduling-plus-operation of aggregated storage fleets. The candidate approaches are described in the following subsections, and comparisons made in Table I. Note that, within each broad approach, we only consider options with feasibility guarantees for practical usability. In addition to the benefits shown in Table I, the DLR representation is a powerful tool for simplification. This will be shown in future work due to space constraints.

1) *DLR framework*: In the scheduling phase, encode the DLR curves into an optimisation problem to determine the reserved total energy E^d . During the operation phase, choose the aggregate power allocation in real time, subject to the equality constraint on total energy and E - p inequality constraints (scalar during recovery), and dispatch the response power over each sample period using the DLR broadcast procedure.

2) *Sequential E - p dispatch*: During initial scheduling, reserve an E - p curve for the fleet (optionally: parameterise this via E^d and choose the maximum-flexibility truncation). Then, during discharge operation, allocate the power response over each sample period, subject to the E - p inequality constraints only, via broadcast dispatch. After discharging operation, transform into recharging coordinates and repeat the process.

3) *Single virtual battery [4]–[7]³*: Choose a fixed set of scalar battery parameters to approximate the fleet, then incorporate this into the scheduling optimisation problem. During operation, allocate a power level for each sample period subject to the scalar constraints on power and energy.

³We consider an inner bound on parameters such that the single virtual battery encoding is guaranteed to result in the allocation of feasible signals

We point out here that it is straightforward to create a feasibility-guaranteeing virtual battery from the DLR curves for a given choice of E^d .

4) *Asymmetric block offers* [14]: Compute a finite set of discharge-recharge offers, each approximating the fleet as a different single virtual battery. Encode all of these offers into an optimisation problem covering the full operational period. During operation, allocate a power level for each sample period subject to the scalar constraints on power and energy.

5) *Full information scheduling* [2], [3]: Ahead of time, use full information for each device to determine an allocation of the fleet as the solution to an optimisation problem covering the full operational period. Dispatch the solution ahead of time.

6) *Full information direct control* [12], [13]: Omit the scheduling phase. In real time, communicate directly with each device to achieve the optimal response.

VI. CONCLUSION AND FUTURE WORK

This paper has presented a framework for the procurement of reserve flexibility with guaranteed recovery. The DLR representation encodes full discharging capabilities and easily interpretable recovery capabilities that exactly account for losses. Feasibility is guaranteed, so that any request deemed admissible based on the purchased reserve can necessarily be met by the fleet. We have provided an example construction of the constituent curves and benchmarked our approach against the state-of-the-art.

In future work, the authors intend to extend these results into settings where cross-charging is allowed to take place. In particular, they aim to investigate the applicability of the DLR framework in such circumstances and characterise any resulting reduction in optimality. In addition, the possibility to use simplified fleet representations (which lead to even more compact DLR representations) will be investigated.

ACKNOWLEDGEMENTS

This work was supported by EPSRC studentship 1688672, by The Alan Turing Institute under the EPSRC grant EP/N510129/1 and by the Lloyd's Register Foundation-Alan Turing Institute programme on Data-Centric Engineering under the LRF grant G0095. The authors would also like to thank the Isaac Newton Institute for Mathematical Sciences for support and hospitality during the programme Mathematics of Energy Systems (EPSRC grant number EP/R014604/1). Special thanks to Pierre Pinson for enlightening discussions on the topic.

APPENDIX

A. Proof of Theorem III.1

Given \tilde{x} , define $\tilde{p} \doteq \sum_{i: x_i \geq \tilde{x}} \bar{p}_i$. Using this, we can write down the capacity curve based on \tilde{x} as follows:

$$\Omega_{\tilde{p}, \tilde{x}}(p) = \begin{cases} \Omega_{\tilde{p}, x}(p), & \text{if } p \geq \tilde{p} \\ \Omega_{\tilde{p}, x}(\tilde{p}) + (\tilde{p} - p)\tilde{x}, & \text{otherwise.} \end{cases} \quad (\text{A.1})$$

In particular, $\Omega_{\tilde{p}, \tilde{x}}(0) = E^d$. We can therefore deduce that

$$\left. \begin{aligned} E_{P^d}(p) &\leq \Omega_{\tilde{p}, x}(p) \quad \forall p \\ E_{P^d}(0) &\leq E^d \end{aligned} \right\} \iff E_{P^d}(p) \leq \Omega_{\tilde{p}, \tilde{x}}(p) \quad \forall p, \quad (\text{A.2})$$

and so the result follows from Property II.5. \square

B. Proof of Theorem IV.1

Consider two fleets of devices: $(\bar{p}^{(1)}, x^{(1)})$ of size n , indexed by descending time-to-go values (i.e. $x_i \geq x_{i+1}$) and $(\bar{p}^{(2)}, x^{(2)})$ that consists of a single device. With slight abuse of notation, we denote the parameters of the latter by $\bar{p}^{(2)}, x^{(2)}$. We define $j : x_j^{(1)} \geq x^{(2)} > x_{j+1}^{(1)}$, with $x_0^{(1)} \doteq x^{(2)}$ and $x_{n+1}^{(1)} \doteq 0$. Now, consider the resultant capacity curve of the combined fleet, as follows:

$$\Omega_{1+2}(p) = \begin{cases} \Omega_1(p) + \bar{p}^{(2)}x^{(2)}, & \text{if } p \leq p' \\ \Omega_1(p - \bar{p}^{(2)}), & \text{if } p \geq p' + \bar{p}^{(2)} \\ \Omega_1(p') + (p' + \bar{p}^{(2)} - p)x^{(2)}, & \text{otherwise,} \end{cases} \quad (\text{A.3})$$

in which $p' \doteq \sum_{i=1}^j \bar{p}_i^{(1)}$. Denote the flexibilities corresponding to the two fleets as \mathcal{F}_1 and \mathcal{F}_2 . Denote their vertices as the sets \mathcal{V}_1 and \mathcal{V}_2 , which are given by

$$\mathcal{V}_1 = \mathcal{C}(\Omega_1) \cup \{(0, +\infty), (+\infty, 0)\}, \quad (\text{A.4a})$$

$$\mathcal{V}_2 = \{(0, +\infty), (0, \bar{p}^{(2)}x^{(2)}), (\bar{p}^{(2)}, 0), (+\infty, 0)\}, \quad (\text{A.4b})$$

in which $\mathcal{C}(\Omega)$ denotes the vertices of a capacity curve $\Omega(\cdot)$. We can then compute the Minkowski sum as follows:

$$\begin{aligned} \mathcal{F}_1^{\mathbb{C}} \oplus \mathcal{F}_2^{\mathbb{C}} &= \text{Conv}(\{a + b : a \in \mathcal{V}_1, b \in \mathcal{V}_2\}) \\ &= \text{Conv}(\{a + b : a \in \mathcal{C}(\Omega_1), b = (0, \bar{p}^{(2)}x^{(2)}), (\bar{p}^{(2)}, 0)\} \\ &\quad \cup \{(0, +\infty), (+\infty, 0)\}), \end{aligned} \quad (\text{A.5})$$

in which $\text{Conv}(\cdot)$ denotes the formation of the convex hull. This returns the corresponding set of vertices

$$\begin{aligned} &\{(\sum_{i=1}^k \bar{p}_i^{(1)}, \sum_{i=k}^n \bar{p}_i^{(1)}x_k + \bar{p}^{(2)}x^{(2)}), k = 0, \dots, j-1\} \\ &\cup \{(\sum_{i=1}^k \bar{p}_i^{(1)} + \bar{p}^{(2)}, \sum_{i=k}^n \bar{p}_i^{(1)}x_k), k = j, \dots, n\} \\ &\cup \{(0, +\infty), (+\infty, 0)\} \\ &= \mathcal{C}(\Omega_{1+2}) \cup \{(0, +\infty), (+\infty, 0)\}, \end{aligned} \quad (\text{A.6})$$

so the result follows for the addition of a single device to a complex fleet. The general result then follows because the Minkowski summation operator is associative. \square

REFERENCES

- [1] "Future Energy Scenarios," National Grid, Tech. Rep., July 2021.
- [2] A. Y. Saber and G. K. Venayagamoorthy, "Resource scheduling under uncertainty in a smart grid with renewables and plug-in vehicles," *IEEE Systems Journal*, vol. 6, no. 1, pp. 103–109, 2012.
- [3] N. G. Paterakis, O. Erdinc, I. N. Pappi, A. G. Bakirtzis, and J. P. Catalao, "Coordinated Operation of a Neighborhood of Smart Households Comprising Electric Vehicles, Energy Storage and Distributed Generation," *IEEE Transactions on Smart Grid*, vol. 7, no. 6, pp. 2736–2747, 2016.
- [4] S. Vandael, B. Claessens, M. Hommelberg, T. Holvoet, and G. Deconinck, "A scalable three-step approach for demand side management of plug-in hybrid vehicles," *IEEE Transactions on Smart Grid*, vol. 4, no. 2, pp. 720–728, jun 2013.
- [5] M. Gonzalez Vaya and G. Andersson, "Optimal Bidding Strategy of a Plug-In Electric Vehicle Aggregator in Day-Ahead Electricity Markets under Uncertainty," *IEEE Transactions on Power Systems*, vol. 30, no. 5, pp. 2375–2385, 2015.

- [6] H. Zhang, Z. Hu, Z. Xu, and Y. Song, "Evaluation of Achievable Vehicle-to-Grid Capacity Using Aggregate PEV Model," *IEEE Transactions on Power Systems*, vol. 32, no. 1, pp. 784–794, 2017.
- [7] Z. Xu, D. S. Callaway, Z. Hu, and Y. Song, "Hierarchical Coordination of Heterogeneous Flexible Loads," *IEEE Transactions on Power Systems*, vol. 31, no. 6, pp. 4206–4216, 2016.
- [8] M. Mazidi, A. Zakariazadeh, S. Jadid, and P. Siano, "Integrated scheduling of renewable generation and demand response programs in a microgrid," *Energy Conversion and Management*, vol. 86, pp. 1118–1127, 2014.
- [9] X. Wang, A. Palazoglu, and N. H. El-Farra, "Operational optimization and demand response of hybrid renewable energy systems," *Applied Energy*, vol. 143, pp. 324–335, 2015.
- [10] K. M. Tsui and S. C. Chan, "Demand response optimization for smart home scheduling under real-time pricing," *IEEE Transactions on Smart Grid*, vol. 3, no. 4, pp. 1812–1821, 2012.
- [11] Z. Wang, C. Gu, F. Li, P. Bale, and H. Sun, "Active demand response using shared energy storage for household energy management," *IEEE Transactions on Smart Grid*, vol. 4, no. 4, pp. 1888–1897, 2013.
- [12] F. Adamek, M. Arnold, and G. Andersson, "On decisive storage parameters for minimizing energy supply costs in multicarrier energy systems," *IEEE Transactions on Sustainable Energy*, vol. 5, no. 1, pp. 102–109, 2014.
- [13] T. Pippia, J. Sijs, and B. De Schutter, "A single-level rule-based model predictive control approach for energy management of grid-connected microgrids," *IEEE Transactions on Control Systems Technology*, vol. 28, no. 6, pp. 2364–2376, 2020.
- [14] N. O'connell, P. Pinson, H. Madsen, and M. O'malley, "Economic Dispatch of Demand Response Balancing Through Asymmetric Block Offers," *IEEE Transactions on Power Systems*, vol. 31, no. 4, pp. 2999–3007, 2016.
- [15] R. R. Appino, V. Hagenmeyer, and T. Faulwasser, "Towards optimality preserving aggregation for scheduling distributed energy resources," *IEEE Transactions on Control of Network Systems*, 2021.
- [16] M. P. Evans, S. H. Tindemans, and D. Angeli, "A graphical measure of aggregate flexibility for energy-constrained distributed resources," *IEEE Transactions on Smart Grid*, vol. 11, no. 1, pp. 106–117, 2020.
- [17] J. Cruise and S. Zachary, "Optimal scheduling of energy storage resources," *Preprint arXiv:1808.05901.05788*, pp. 1–19, 2018.
- [18] M. P. Evans, D. Angeli, G. Strbac, and S. H. Tindemans, "Chance-constrained ancillary service specification for heterogeneous storage devices," in *2019 IEEE PES Innovative Smart Grid Technologies Europe (ISGT-Europe)*, 2019, pp. 1–5.
- [19] "Ancillary Services," PJM, 2017, <http://www.pjm.com/markets-and-operations/ancillary-services.aspx>.
- [20] "Load Participation and Demand Response," CAISO, 2017, <http://www.caiso.com/participate/Pages/Load/Default.aspx>.
- [21] "Balancing Services," National Grid, 2020, <https://www.nationalgrideso.com/balancing-services>.
- [22] V. Trovato, S. H. Tindemans, and G. Strbac, "Leaky storage model for optimal multi-service allocation of thermostatic loads," *IET Generation, Transmission & Distribution*, vol. 10, no. 3, pp. 585–593, 2016.
- [23] H. Hao, B. M. Sanandaji, K. Poolla, and T. L. Vincent, "Aggregate flexibility of thermostatically controlled loads," *IEEE Transactions on Power Systems*, vol. 30, no. 1, pp. 189–198, 2015.
- [24] L. Zhao, W. Zhang, H. Hao, and K. Kalsi, "A Geometric Approach to Aggregate Flexibility Modeling of Thermostatically Controlled Loads," *IEEE Transactions on Power Systems*, vol. 32, no. 6, pp. 4721–4731, 2017.
- [25] S. Kundu, K. Kalsi, and S. Backhaus, "Approximating flexibility in distributed energy resources: A geometric approach," in *20th Power Systems Computation Conference, PSCC 2018*. Power Systems Computation Conference, 2018, pp. 1–7.
- [26] S. Zachary, S. H. Tindemans, M. P. Evans, J. R. Cruise, and D. Angeli, "Scheduling of energy storage," *Philosophical Transactions of the Royal Society A: Mathematical, Physical and Engineering Sciences*, vol. 379, no. 2202, p. 20190435, 2021.
- [27] M. Evans, S. H. Tindemans, and D. Angeli, "Robustly maximal utilisation of energy-constrained distributed resources," in *2018 Power Systems Computation Conference (PSCC)*, 2018, pp. 1–7.
- [28] M. P. Evans, S. H. Tindemans, and D. Angeli, "Minimizing unserved energy using heterogeneous storage units," *IEEE Transactions on Power Systems*, vol. 34, no. 5, pp. 3647–3656, 2019.